Deciphering sources of U contamination using isotope ratio signatures in the Loire River sediments: exploring the relevance of 233 U/ 236 U and stable Pb isotope ratios

Amandine Morereau, Hugo Jaegler, Karin Hain, Peter Steier, Robin Golser, Aurélien Beaumais, Hugo Lepage, Frederique Eyrolle, Cécile Grosbois, Charlotte Cazala, et al.

Deciphering sources of U contamination using isotope ratio signatures in the Loire River sediments: exploring the relevance of $^{233}U/^{236}U$ and stable Pb isotope ratios

Amandine Morereau[1], Hugo Jaegler[1], Karin Hain[2], Peter Steier[2], Robin Golser[2], Aurélien Beaumais[1], Hugo Lepage[1], Frédérique Eyrolle[1], Cécile Grosbois[3], Charlotte Cazala[1], Alkiviadis Gourgiotis[1]*

[1]Institut de Radioprotection et de Sûreté Nucléaire (IRSN), PSE-ENV/SRTE/LRTA, SEDRE/LELI, BP 3, 13115 Saint-Paul-Lez-Durance, France

[2]Faculty of Physics, Isotope Physics, University of Vienna, Währinger Str. 17, 1090 Vienna, Austria

[3]Université de Tours, EA 6293 Géohydrosystèmes continentaux (GéHCO), Parc de Grandmont, 37200 Tours Cedex, France

*Corresponding author: alkiviadis.gourgiotis@irsn.fr

Abstract

A broad range of contaminants has been recorded in sediments of the Loire River over the last century. Among a variety of anthropogenic activities of this nuclearized watershed, extraction of uranium and associated activities during more than 50 years as well as operation of several nuclear power plants led to industrial discharges, which could persist for decades in sedimentary archives of the Loire River. Highlighting and identifying the origin of radionuclides that transited during the last decades and were recorded in the sediments is challenging due to i) the low concentrations which are often close or below the detection limits of routine environmental surveys and ii) the mixing of different sources. The determination of the sources of anthropogenic radioactivity was performed using multi-isotopic fingerprints ($^{236}U/^{238}U$, $^{206}Pb/^{207}Pb$ and $^{208}Pb/^{207}Pb$) and the newly developed $^{233}U/^{236}U$ tracer. For the first time $^{233}U/^{236}U$ data in a well-dated river sediment core in the French river Loire are reported here. Results highlight potential sources of contamination among which a clear signature of anthropogenic inputs related to two accidents of a former NUGG NPP that occurred in 1969 and 1980. It is important to mention that the ^{233}U and ^{236}U levels measured in this work by recent high performance analytical methods are at ultra-trace levels and present a negligible radiological impact on health and on the environment. The determination of the mining activities by the use of stable Pb isotopes is still challenging probably due to the limited dissemination of the Pb-bearing material marked by the U-ore signature downstream to the former U mines.

Keywords: ^{233}U, ^{236}U, nuclear power plant, uranium mines, Loire River, lead isotopes

Introduction

The Loire River is the longest French river with a linear distance of 1,012 km between its source (Mont Gerbier-de-Jonc) and its entrance into the estuary (Ancenis). Its watershed covers an area of 117,800 km², which represents 20% of the surface area of metropolitan France (Coularis, 2016; Dhivert, 2014). The Loire basin is geologically rich in uranium-bearing rocks and has been exploited for more than 50 years (since 1947) to extract the uranium necessary for the manufacture of nuclear fuel (IRSN, 2019). In the Loire watershed, 64,000 tons of uranium were produced between 1947 and 2002, i.e., around 80% of total French production (IRSN, 2019). A total of 138 mining installations are located in the Loire basin, all located in the southern part of the basin, with the most uranium-rich rocks (Ielsch et al., 2017) (Figure 1). Moreover, the Loire River is one of the most nuclearized rivers in Europe since the 1960s, especially by the construction of Nuclear Power Plants (NPP) first equipped with reactors from the Natural Uranium Graphite Gas (NUGG) sector, then with Pressurized Water Reactors (PWRs). The NUGG reactors were set up along the Loire River between 1963 (Chinon) and 1971 (Saint-Laurent-des-Eaux). In 1980, the first PWR was commissioned (Dampierre) and PWRs gradually replaced the NUGG reactors. In 1969 and 1980, two nuclear accidents took place at the former Saint-Laurent-des-Eaux NPP (NUGG reactors named SLA1 and SLA2 respectively). These events led to the fusion of fuel elements and plutonium was detected in water and sediment in the Loire River (Eyrolle et al., 2019; Guignard and Catoire, 2015; IRSN, 2016; Thomas, 1982). All NUGG reactors located on the Loire watershed were definitely stopped in 1992. Today, 4 NPPs are located along the Loire River and 1 NPP on the Vienne tributary (on the downstream part of the Loire River). These NPPs are equipped with PWRs and are currently in operation (Figure 1).

Operations in both U mining sites and NPPs can lead to radionuclide releases increasing their concentration in the environment. Several studies were performed in order to retrace the historical evolution and the origin of various radionuclides transiting along the Loire River during the last century (Copard et al., 2021; Eyrolle et al., 2019). Nevertheless, the uranium and lead from nuclear activities which were transferred along the Loire River since the beginning of the nuclear age remain poorly documented. This study was part of the PALYNO (NEEDS - Environment) and TRAJECTOIRE (ANR) projects which aim at establishing the socio-historical trajectories of key non-legacy contaminants (radionuclides, microplastics and ultra-rare metals) on the major French watersheds based on the observations (data sets) of the last decades. For this purpose, multi-isotopic tracers were determined in the same sediment core collected downstream the Loire River Basin and covering a large period of time, i.e. from the 1930s to present day. Four isotopic ratios were used to trace anthropogenic origins of uranium and lead: $^{236}U/^{238}U$, $^{233}U/^{236}U$, $^{206}Pb/^{207}Pb$ and $^{208}Pb/^{207}Pb$.

The $^{236}U/^{238}U$ ratio is a powerful indicator to quantify the contributions of uranium from anthropogenic origin. The ^{236}U is mainly produced by neutron capture on ^{235}U and allow us to efficiently highlight small anthropogenic U contributions that are completely undetectable by using conventional methods based on naturally occurring U isotopes (^{238}U, ^{235}U, ^{234}U) fingerprinting. Three main sources of ^{236}U can be distinguished in the environment: global fallout from past nuclear testing, nuclear accidents and authorized discharges of spent nuclear fuel reprocessing plants. The global inventory and the relative contribution of these sources in the environment is still to be understood and some works have been involved in this effort (Casacuberta et al., 2014; Sakaguchi et al., 2009) .The natural $^{236}U/^{238}U$ ratios in the pre-anthropogenic environment range from 10^{-14} to 10^{-10}, the typical value of the $^{236}U/^{238}U$ ratio for U-ores ranges between 10^{-12} and 10^{-10} (Steier et al., 2008; Wilcken et al., 2008). Areas influenced by anthropogenic ^{236}U display $^{236}U/^{238}U$ ratio values greater than 10^{-9}: from 10^{-6} to more than 10^{-3} near the Chernobyl damaged NPP (Boulyga and Becker, 2001; Hotchkis et al., 2000; Mironov et al., 2002), from 10^{-8} to 10^{-6} near the Fukushima one (Jaegler et al., 2019; Sakaguchi et al., 2014; Shinonaga et al., 2014; Yang et al., 2019, 2016), from 10^{-6} to 10^{-5} in the sediments from the Irish Sea impacted by the Sellafield reprocessing plant (Hotchkis et al., 2000; Ketterer et al., 2003; Marsden et al., 2001; Srncik et al., 2011a) and about 10^{-9} to 10^{-6} in areas affected by the global fallout from past nuclear testing as is the case in the northern hemisphere (Quinto et al., 2013, 2009; Sakaguchi et al., 2010, 2009; Shao et al., 2019; Srncik et al., 2011b). Moreover, the $^{236}U/^{238}U$ isotopic ratio was widely used to trace water masses in oceans (Casacuberta et al., 2014; Christl et al., 2015; Sakaguchi et al., 2012). However, the large range of $^{236}U/^{238}U$ variation can sometime lead to signature overlapping making thus difficult the identification of the U origin. Besides, it is worth mentioning that $^{236}U/^{238}U$ variation depends also to natural variations of ^{238}U.

A second useful anthropogenic U isotope for environmental studies is ^{233}U. This isotope has been measured by Accelerator Mass Spectrometry (AMS) in samples impacted by nuclear weapons and close to contaminated sites (Child and Hotchkis, 2013; Tumey et al., 2009). Recent pioneering works at the Vienna Environmental Research Accelerator (VERA) allowed very low-level measurements of ^{233}U in environmental samples by AMS (Hain et al., 2020, 2017). Thanks to these studies, the $^{233}U/^{236}U$ ratio became a new powerful tracer, combining two anthropogenic isotopes emitted simultaneously in different proportions from the above described sources, allowing to discriminate environmental emissions of civil nuclear activities from global fallout (Hain et al., 2020, 2017; Qiao et al., 2021, 2020). This tracer, independent of natural ^{238}U variations, offers also new perspectives as a new oceanic tracer (Lin et al., 2021). In brief, the main source for anthropogenic ^{233}U is nuclear weapons (global atmospheric fallout), either directly released by ^{233}U fueled weapons or produced in

thermonuclear weapons by the $^{235}U(n,3n)^{233}U$ reaction. This reaction requires fast neutrons and highly enriched U in contrast to nuclear power plants for which thermal neutrons are needed for the fission of ^{235}U. On the other hand the ^{236}U can be produced by both nuclear power plants and fission and thermonuclear weapons. Hain et al. (2020) estimated an average value of the $^{233}U/^{236}U$ ratio from global fallout equal to $(1.40 \pm 0.15) \times 10^{-2}$. Reactor model calculations obtained for the fuel of pressurized water reactors give an average $^{233}U/^{236}U$ close to $\sim 10^{-7}$ (Naegeli, 2004). Therefore, any actual $^{233}U/^{236}U$ atomic ratios below $(1.40 \pm 0.12) \times 10^{-2}$ for natural samples would indicate the admixing of reactor-associated ^{236}U. In the Irish Sea, an average $^{233}U/^{236}U$ atomic ratio of $(0.12 \pm 0.01) \times 10^{-2}$ has been measured by Hain et al. (2020), reflecting a dominant reactor signal released from Sellafield. These results clearly show that this isotope ratio could be used to discriminate the different uranium sources in the environment.

Following the pioneering work of Clair Patterson on the identification of Pb air pollution sources (C.C Patterson and Settle, 1987; Clair C Patterson and Settle, 1987), lead isotopes have been widely used for environmental studies allowing identifying sources of lead pollution (Komárek et al., 2008). Lead isotopes have been also studied in a number of French rivers such as the Loire River (Négrel and Petelet-Giraud, 2012) and the Seine River (Ayrault et al., 2012). Monna et al. (1997) identified Pb isotope ratio end-members of airborne particulate material in France. In the context of environmental impact assessment studies related to uranium mining activities, Pb isotopes constitute a relevant tracer. Indeed, the enriched ^{238}U and ^{235}U contents in U-ores lead to the production of radiogenic ^{206}Pb and ^{207}Pb with ^{206}Pb being the most abundant isotope. In contrast, the low Th contents of U-ores lead to a restricted production of ^{208}Pb, generating thus a major contrast between the isotopic signatures of the U-ores and that of the Earth crust (hereafter, Present Day Average Crustal (PDAC) (Cumming and Richards, 1975; Stacey and Kramers, 1975)) for which ^{208}Pb is the most abundant isotope. It is worth mentioning that the Pb isotope signature of U-ores is also markedly different from that of industrial lead and that from gasolines for which ^{208}Pb is also the most abundant isotope. ^{204}Pb is not a radiogenic isotope, and thus its concentration does not evolve on Earth over time. The isotopes of lead were used in several environmental impact assessment studies of uranium mining sites or unexploited uranium deposits (Bollhöfer, 2012; Bollhöfer et al., 2006; Bollhöfer and Martin, 2003; Dang et al., 2018; Frostick et al., 2011, 2008; Gulson et al., 1989; Kyser et al., 2015; Liu et al., 2018; Munksgaard et al., 2003; Santos and Tassinari, 2012; Vecchia et al., 2017) and although roughly 250 sites were operated in France (IRSN, 2019) only three published works deal with Pb isotopes (Cuvier et al., 2016; Gourgiotis et al., 2020; Martin et al., 2020). Mining activities (dewatering water, emission of dust, wastewaters from tailings storage basins, etc.) or even natural phenomena of weathering of the deposit, particularly in the case of unexploited deposits

(e.g. erosion, leaching), contribute also to the transport of Pb coming from the U-ore (hereafter marked as Pb*) outside the deposit (Kister et al., 2004).

This work aims to investigate past major contamination events which occurred during the last seventy years of development of nuclear industries from mining to accidental releases of radionuclides by nuclear power plants. The originality of this study is to combine the newly developed $^{233}U/^{236}U$ tracer, $^{236}U/^{238}U$ and associated lead isotopes. Although the former Saint-Laurent-des-Eaux NUGG NPP accidents resulted in well-known contamination of waters and sediments of the Loire River by accidental discharges of plutonium (IRSN, 2016; Thomas, 1982), any study of these ratios had been carried out so far on this river. Data of ^{233}U and ^{236}U isotopes were explored to evaluate the relevance of this tracer to distinguish emissions of civil nuclear industry from weapons fallout while lead isotopes were used as a potential tracer to highlight uranium mining and milling activities.

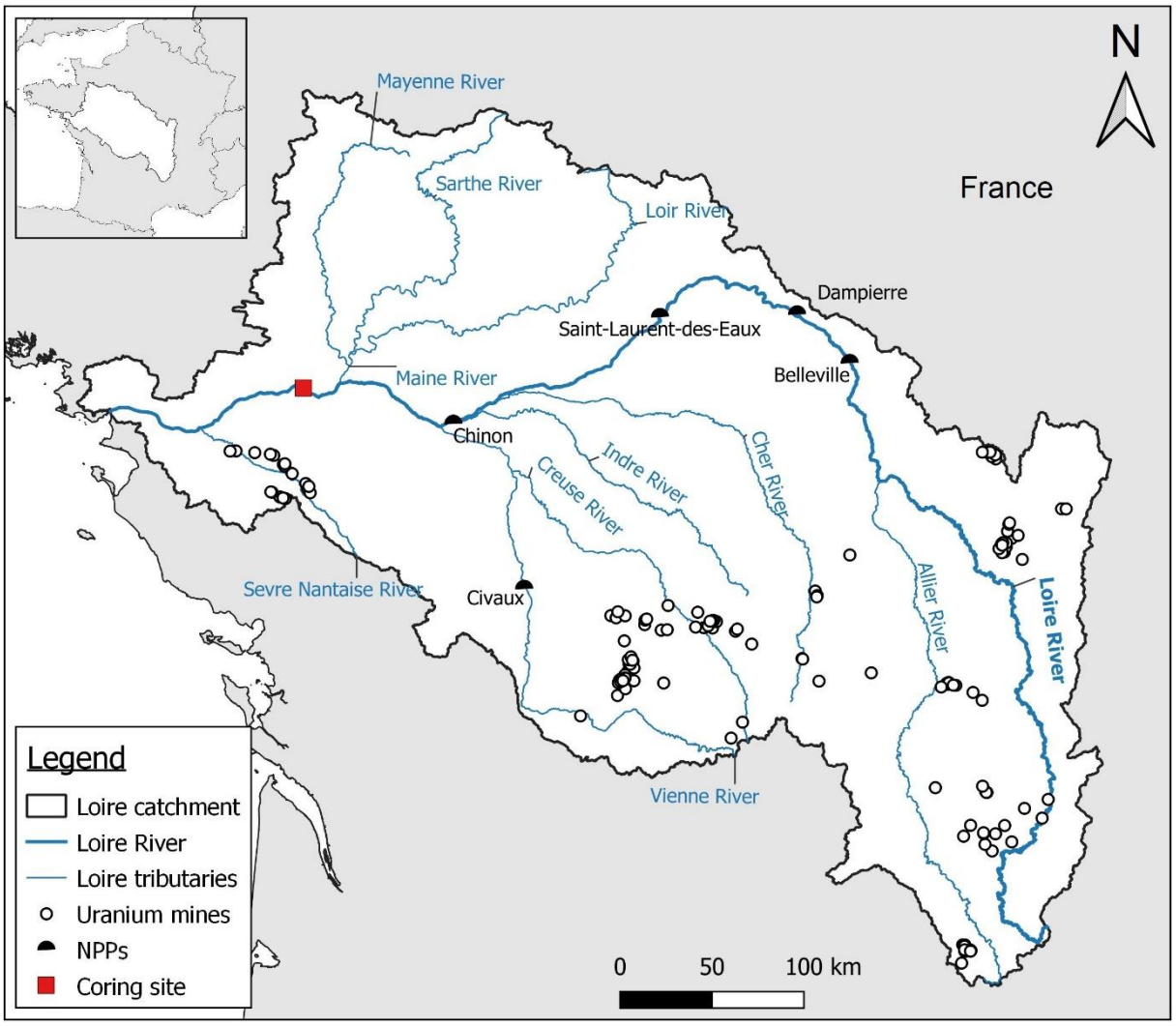

Figure 1: Map of uranium mines, NPPs and coring site locations in the Loire River catchment in France.

Materials and methods

Sediment core sampling and dating.

The sampling site is located at coordinates 47 ° 23'34.0 "N 0 ° 51'23.1" W, on an alluvial island in the town of Montjean-sur-Loire (France), which is located downstream all the Loire and Vienne NPPs and most of uranium mines (Figure 1), but upstream of the estuary thus outside the influence of the tides of the Atlantic Ocean. The coring site, at an altitude of 12 to 17 m, is submerged only during flood events for the last decade, when the flow of the Loire exceeds 2,500 m^3/s (the average annual flow of the Loire at the station of Montjean-sur-Loire is 840 m^3/s). This sampling area, described by Grosbois et al. (2012), is considered to be a coring site suitable for historical tracing of contamination due to the sedimentary accumulation of fine particles during flood episodes thanks to the presence of vegetation which slows down the currents and favours the deposition of fine material. To obtain the final master core, several one-meter sediment cores were collected in September 2016, using a percussion driller (Cobra TT, SDEC, France) with transparent PVC tubes (diameter 46 mm). Once in the laboratory, 5 cm slices were stored at -25°C and freeze-dried under dehydrated nitrogen flux in order to avoid any atmospheric exchange and sieved at 2 mm before analyses. The age model is based on ^{137}Cs concentrations and $^{238}PU/^{239}Pu$ activity ratio. Radiocesium concentrations show two major peaks at 92.5 cm and 37.5 cm related to the peak of radioactive emissions from atmospheric nuclear tests in 1963 and to the radioactive fallout from the Chernobyl accident in 1986 respectively. In addition, plutonium isotopes ($^{238}Pu/^{239+240}Pu$ activity ratio) also show two peaks, the first one at 77.5 cm and the second one at 52.5 cm. Although these isotopes were released during atmospheric nuclear tests over the 1945 - 1980 period and the explosion of the Transit 5 BN-3 satellite in 1964, plutonium isotopes ratios observed in the particular case of the Loire River are due to accidental liquid discharges of plutonium by the Saint-Laurent-des-Eaux NPP in 1969 (77.5 cm depth) and 1980 (52.5 cm depth). It is important to note that in the case of fluvial environments, the sedimentation rate is variable over time contrary to lakes and quiet environments. Consequently, the $^{210}Pb_{xs}$ dating method is not available in this study as previously mentioned in Grosbois et al. (2012), Eyrolle et al. (2019), Morereau (2020) and Copard et al. (2021). Hence, these identified chronological landmarks (1963, 1969, 1980 and 1986) allow obtaining a robust age model presenting two main periods with constant sedimentation rates, the 1963 – 1986 period with 2.4 ± 0.2 cm/y and the 1986 – 2016 period with 1.3 ± 0.2 cm/y with uncertainties estimated to ± 2 years.

Chemical preparation of samples.

High-purity acids were obtained by distillation (Savillex® DST-1000 system) of hydrochloric acid (HCl, Merck, Emsure 37%), nitric acid (HNO_3, VWR Chemicals, Normapur 68%). De-ionized water was

produced by a Millipore system (18.2 MΩ/cm resistivity). All sample dilutions and solutions for elemental and isotope analysis were performed with 0.5 mol/L (M) HNO_3. This acid was also used as the blank and for instrument washing between standards and samples.

For isotopic analysis, ~ 10 g of finely ground dry samples were calcined in an oven at 480°C for 52h in view of the realization of chemical separations in order to extract uranium and lead prior to the measurement steps. After calcination, the samples were transferred to the Teflon vials (Savillex) and aqua regia has been added to the dry residue. The mix was heated at 90 °C for 10 h in closed vials and after it had cooled down, the solution was filtered using a disposable filter set of 0.45 µm porosity. The insoluble residue was discarded and the filtrate was collected to the same vials and evaporated to dryness before adding 2 mL of 3 M (mol/L) of HNO_3. Then, the uranium was separated from the sample matrix using UTEVA resin (TrisKem International) previously conditioned in 3 M HNO_3 (Douville et al., 2010): after sample loading onto the columns, the resin was rinsed with 3 M HNO_3 to eliminate the sample matrix. This fraction was collected for Pb isotope analysis. Then the resin was rinsed with 3 M HCl for Th elution and U was finally eluted with 0.1 M HCl. U fractions were evaporated to dryness and then taken up in HNO_3 0.05 M. Five selected U samples were split in two parts, one for ICP-MS/MS analysis and one for analysis by AMS. While samples are ready for ICP-MS/MS analysis then, AMS analysis requires the preparation of solid material from the sample aliquots.

For this aim, 1-2 mg of Fe and 1 mL NH_3 20% (VWR, ultrapure, Pennsylvania, United States) were added to the solution. The precipitate is separated from the supernatant by centrifugation, then evaporated in an oven during 4h at 90°C. Iron oxide samples containing the uranium fractions were then placed in an electric furnace at 800°C during 3h. Finally, iron oxide samples were pressed into aluminum sample holders for AMS analyses (Lin et al., 2021; Steier et al., 2019).

Elution fractions containing Pb were evaporated to dryness and redissolved in 0.3 mL of HBr (0.5 M, Ultrapur) for Pb separation and purification by ion-exchange resin (Biorad, AG 1-X8, 200-400 mesh). The resin was previously washed (0.25 M HNO_3 and HCl 0.2 M) and conditioned with 0.5 M HBr. In short, the protocol (Manhes et al., 1984) consists of the sample load onto the column, a matrix wash with ~5 mL of HBr (0.5 M), and Pb elution with ~5 mL of HCl (0.2 M). Then, the samples were evaporated to dryness and taken up in HNO_3 0.5 M for ICP-MS/MS analysis.

Uranium and lead isotope analysis by ICP-MS/MS.

Lead and $^{236}U/^{238}U$ isotope ratio measurements were performed using an Agilent 8800 ICP-MS/MS (Agilent Technologies, Tokyo, Japan) housed at the LELI laboratory of the French Institute of

Radiological Protection and Nuclear Safety (PATERSON mass spectrometry Platform, IRSN, Fontenay-aux-Roses, France).

In short, for $^{236}U/^{238}U$ ratio analysis the ICP-MS/MS was coupled with an efficient desolvating module (APEX Ω, Elemental Scientific) and all measurements were performed in MS/MS mass shift mode. N_2O was introduced in the collision reaction cell and uranium was analyzed in UO^+ form. This configuration significantly decreased uranium hydride formation ($^{235}UH^+$) as well as ^{238}U and ^{235}U peak tailing allowing an accurate determination of low $^{236}U/^{238}U$ isotope ratios. Detailed information about $^{236}U/^{238}U$ measurements by ICP-MS/MS can be found in Jaegler et al. (2020).

For lead isotope analysis ($^{206}Pb/^{207}Pb$ and $^{208}Pb/^{207}Pb$) the ICP-MS/MS was run in single quadrupole mode, and a Peltier-cooled (2°C) Scott-type spray chamber with a PFA nebulizer (0.33 mL/min, ESI, U.S.) was used as the introduction system. The self-aspiration mode was used for the sample introduction and all analyses were performed in pulse counting mode. More details about lead isotope ratio measurements can be found in Gourgiotis et al. (2020). ICP-MS/MS data can be found in Table 1.

AMS analysis.

The AMS measurement of $^{236}U/^{238}U$ and $^{233}U/^{238}U$ atomic ratios was carried out at the Vienna Environmental Research Accelerator (VERA) facility at the University of Vienna. A detailed description of the method and configuration for the AMS measurement of ^{236}U and ^{233}U at VERA has been reported in Hain et al. (2020) and Steier et al. (2019). The overall detection efficiency of the system for U atoms in the sputter target was 5×10^{-4} (Steier et al., 2019) assuming complete consumption of the sputter material. The majority of the measurement time was dedicated to the less abundant ^{233}U, while ^{236}U was measured shorter, and the whole material usually was not used up. In general, ^{233}U sample count rates are roughly one order of magnitude above instrumental and procedural blank. AMS data can be found in Table 1.

Gamma spectrometry.

For the gamma spectrometry, samples were beforehand freeze-dried and packed into tightly closed plastic boxes (17-60 mL). They were placed under vacuum in a hermetically sealed bag preventing any exchange of air and light with the outside which could interfere with the secular equilibrium of the radionuclides. The gamma emitters were measured using high resolution and low-background Germanium Hyper pure detectors in the LMRE laboratory of the French Institute of Radiological Protection and Nuclear Safety in Orsay (Bouisset and Calmet, 1997). Only ^{238}U was presented here which was measured from its decay products assuming secular equilibrium. Gamma spectrometry data can be found in Table 1.

262

Table 1: Isotope ratios, concentrations and activities of the samples of the sediment core. Uncertainties are expressed for a coverage factor k=2. Values of ($^{238}Pu/^{239+240}Pu$) in the sediment core and in atmospheric deposit are from Eyrolle et al. (2019). The PADC (Present Day Average Crustal) is from Stacey and Kramers (1975).

Average depth (cm)	Year	$^{236}U/^{238}U$ (x10^{-8})		$^{233}U/^{236}U$ (x10^{-2})	^{238}U	^{236}U (x10^{8})	(^{236}U)	(^{233}U)	$^{204}Pb/^{207}Pb$	$^{206}Pb/^{207}Pb$	$^{208}Pb/^{207}Pb$	($^{238}Pu/^{239+240}Pu$)	($^{238}Pu/^{239+240}Pu$)
		ICP-MS/MS	AMS	AMS	(µg/g) gamma sp.	(atoms/g)	(µBq/kg)					Sediment core	Atmospheric deposit
2.5	2011	0,94 ±0,07	0,96 ±0,07	0,29 ±0,13					0,06419 ±0,0003	1,182 ±0,004	2,460 ±0,006		0,031
17.5	2002				5,6 ±0,6								0,032
27.5	1994				5,5 ±0,6							0,0362	0,034
37.5	1986	1,32 ±0,09	1,18 ±0,12	0,78 ±0,11	5,6 ±0,6	1,85 ±0,24	174 ±22	199 ±37	0,06415 ±0,0004	1,163 ±0,003	2,441 ±0,007	0,0362	0,036
42.5	1984	1,34 ±0,05											0,037
47.5	1982	1,43 ±0,05			5,6 ±0,6	2,05 ±0,23	192 ±22					0,0628	0,037
52.5	1980	1,83 ±0,09	1,86 ±0,15	0,23 ±0,05	5,7 ±0,6	2,65 ±0,31	249 ±29	83 ±20	0,06402 ±0,0004	1,163 ±0,004	2,440 ±0,008	0,0782	0,038
57.5	1978				5,8 ±0,6							0,0681	0,038
62.5	1976				5,9 ±0,6								0,039
67.5	1973	2,28 ±0,09			6,0 ±0,6	3,44 ±0,39	322 ±37						0,040
72.5	1971				5,9 ±0,6							0,0449	0,039
77.5	1969	2,43 ±0,06			5,9 ±0,6	3,61 ±0,39	339 ±36					0,0572	0,037
82.5	1967				5,8 ±0,6							0,0506	0,030
87.5	1965				5,8 ±0,6							0,0276	0,025
92.5	1963	2,15 ±0,16	2,20 ±0,47	0,44 ±0,15					0,06393 ±0,0004	1,170 ±0,003	2,452 ±0,006		0,025
102.5	1959				6,6 ±0,7					1,181 ±0,004	2,462 ±0,006	0,0201	0,026
112.5	1954				6,2 ±0,6							0,0180	
122.5	1950	0,34 ±0,09	0,25 ±0,03	2,49 ±0,59	5,7 ±0,6	0,49 ±0,14	46 ±13	168 ±64	0,06417 ±0,0003	1,177 ±0,003	2,453 ±0,007		
PDAC										1.197	2.472		

Results and discussion

The $^{236}U/^{238}U$ shows anthropogenic sources of uranium.

The measurements of $^{236}U/^{238}U$ isotope ratio were carried out onto 9 samples distributed mainly in the central core layers covering the period between 1950 and 1990. The top layer of the archive (2011) represents the reference value of the current levels and the sample of the bottom of the core (1950) the value before the NPPs activities in the Loire River (first reactors in the Loire River starting from 1963). Some of these samples were also analyzed by both ICP-MS/MS and AMS in order to validate the performance of the recently developed method for $^{236}U/^{238}U$ ratio analysis by ICP-MS/MS (Jaegler et al., 2020). As can be seen in Figure 2, both techniques show similar results within analytical uncertainties.

Activity ratios of Pu from Eyrolle et al. (2019), have been used in this study in order to highlight the accidental releases that occurred in 1969 and 1980 from the former NUGG reactors of the Saint-Laurent des Eaux NPP. These values, higher than the theoretical background ($^{238}Pu/^{239+240}Pu$) ratios as calculated by the authors, are clearly related to the two NUGG NPP events as mentioned above (Figure 2c) (Eyrolle et al., 2019).

The $^{236}U/^{238}U$ ratios range between 0.34×10^{-8} and 2.43×10^{-8} (Figure 2a) and as ^{238}U concentration remains almost constant in these sediment layers, this ratio fluctuation is due to ^{236}U variation only (Figure 2b). It's worth mentioning that ^{238}U concentrations are within natural values variation. The lowest value was measured at the 122.5 cm average depth of the core, dated back to 1950. This layer should be slightly influenced by anthropogenic ^{236}U considering the small number of weapon tests before this year (only 9 tests performed (Mikhailov et al., 1999)) or by ^{236}U downward migration in the core. Indeed, the lowest value, measured in 1950, doesn't reach expected pre-nuclear values $< 10^{-12}$ (Steier et al., 2008).

From 1950 to 1969 a clear increase of the $^{236}U/^{238}U$ ratio was observed with the maximum value in 1969 (2.43×10^{-8}). This high value could correspond to the first event of the Saint-Laurent-des-Eaux NUGG NPP, as pointed out by Pu isotopes. Indeed, the fact that the $^{236}U/^{238}U$ ratio in 1969 is higher than the value in 1963 (maximum contribution of the global fallout), indicates the possibility of a second source of ^{236}U. From 1969 onwards, the $^{236}U/^{238}U$ ratio decreases to reach the current value of 9.4×10^{-9} (2011) with a slope break in 1980 (1.83×10^{-8}) corresponding probably to the second NPP event according to the Pu isotopes (Figure 2a and 2c). Indeed, no more significant direct global fallout occurred and, thus, a second input of ^{236}U should be considered in 1980. From 1983 onwards, the $^{236}U/^{238}U$ ratio doesn't reach the value recorded in 1950 meaning that the additional ^{236}U might originate from the redeposition of global fallout-derived uranium and/or uranium from the former

NUGG reactors of the Saint-Laurent-des-Eaux events which was deposited elsewhere and subsequently resuspended. In this case study it is worth mentioning that the $^{236}U/^{238}U$ signature is not a relevant tracer to highlight U-mine inputs due to the high values of anthropogenic ^{236}U.

In systems affected by different anthropogenic sources (e.g. global fallout and NPP accident), the lack of a second anthropogenic uranium isotope is a disadvantage compared to plutonium for the source identification: $^{236}U/^{238}U$ ratio variation depends on the dilution with natural U. For the Loire River, it is clear that the $^{236}U/^{238}U$ ratio variation fits within the global fallout range (10^{-9} to 10^{-6}) (Alam et al., 2021; Liu et al., 2020; Quinto et al., 2013; Sakaguchi et al., 2010, 2009; Srncik et al., 2011a; Wang et al., 2021; Yang et al., 2019), thus making a reliable identification of possible other U emission sources challenging.

The $^{233}U/^{236}U$ allows discriminating environmental emissions of civil nuclear activities from global fallout.

The ^{233}U isotope was analyzed in order to explore the application of the $^{233}U/^{236}U$ signature in the context of the present work. This isotope ratio stays undisturbed by chemical fractionation in the environment as well as during sample preparation, simplifying the interpretation of the measurement results in the presence of mixing and dilution processes (Child and Hotchkis, 2013). The $^{233}U/^{236}U$ ratio of the layer dated back to 1950 showed a value of $(2.49 \pm 0.6) \times 10^{-2}$ which is higher compared to the average value for the global fallout $(1.40 \pm 0.15) \times 10^{-2}$ (Hain et al., 2020) (Figure 2a). According to the work of Hain et al. (2020) two phases of nuclear weapon testing can be distinguished (1952-1958 and 1961-1962) and a $^{233}U/^{236}U$ ratio of $(5.1 \pm 1.1) \times 10^{-2}$ was obtained by the authors for the earlier phase. Higher values than the average $^{233}U/^{236}U$ global fallout ratio have also been found in Baltic Sea sediments ($^{233}U/^{236}U \approx 0.1$) (Lin et al., 2021) and in a sediment core taken at the continental slope of the Philippine Sea off Mindanao Island ($^{233}U/^{236}U_{max} = (3.47 \pm 0.62) \times 10^{-2}$) (Qiao et al., 2022). Therefore, considering precision of the age model the age (± 2 years), analytical uncertainties and also a potential slight downward migration of anthropogenic U (^{238}U detrital is not influenced by migration), this point fits with the earlier phase of the nuclear weapon testing. The other four points (from 1963 to 2011) indicate the influence of NPP-derived U. Even in the layer corresponding to the peak of the global fallout (1963), the isotope signature is clearly influenced by a NPP signature, probably due to a downward migration of the ^{233}U and ^{236}U isotopes arising from the event in 1969. Similar processes of ^{236}U downward migration have already been observed in an ombrotrophic peat core (Quinto et al., 2013) and in marine sediments (Qiao et al., 2022). It should be noted that for the NPP accidents, our values were compared with the $^{233}U/^{236}U$ signature measured in sediments in the Irish Sea close to the reprocessing Sellafield plant as determined by Hain et al. (2020). This value was found to be equal to

$(0.12 \pm 0.01) \times 10^{-2}$ (marked by vertical dashed line in Figure 2a) and according to the authors reflect a dominant reactor signal released from Sellafield.

It is important to point out that thanks to the $^{233}U/^{236}U$ tracer we can show that even after the second event in 1980, a contribution of civil nuclear U completely "blind" to the ^{238}U concentration (Figure 2 b), is recorded in the sediment core in 1986. Civil nuclear U is also measured in 2011 and this contribution may be explained, again, by: i) the resuspension of past contaminated particles along the Loire River and/or ii) post-depositional upward anthropogenic U migration in the core. However, based on the $^{233}U/^{236}U$ ratio in 2011, the presence of a potential additional source of anthropogenic U at ultra-trace level, i.e. far below the detection limit of conventional analytical methods, cannot be excluded. As this hypothesis is based only on a single measurement point, future studies are needed to further assess it, e.g. by analyzing surface sediments and river water in the vicinity of NPPs. It is important to mention that the ^{233}U and ^{236}U levels measured in this work present a negligible radiological impact on health and on the environment: the highest activities for ^{233}U and ^{236}U were found to be 2×10^{-4} Bq/kg and 3.4×10^{-4} Bq/kg, respectively. These activities are to be compared with the natural ^{238}U activity of the core which is ~68 Bq/kg (~5.5 ppm).

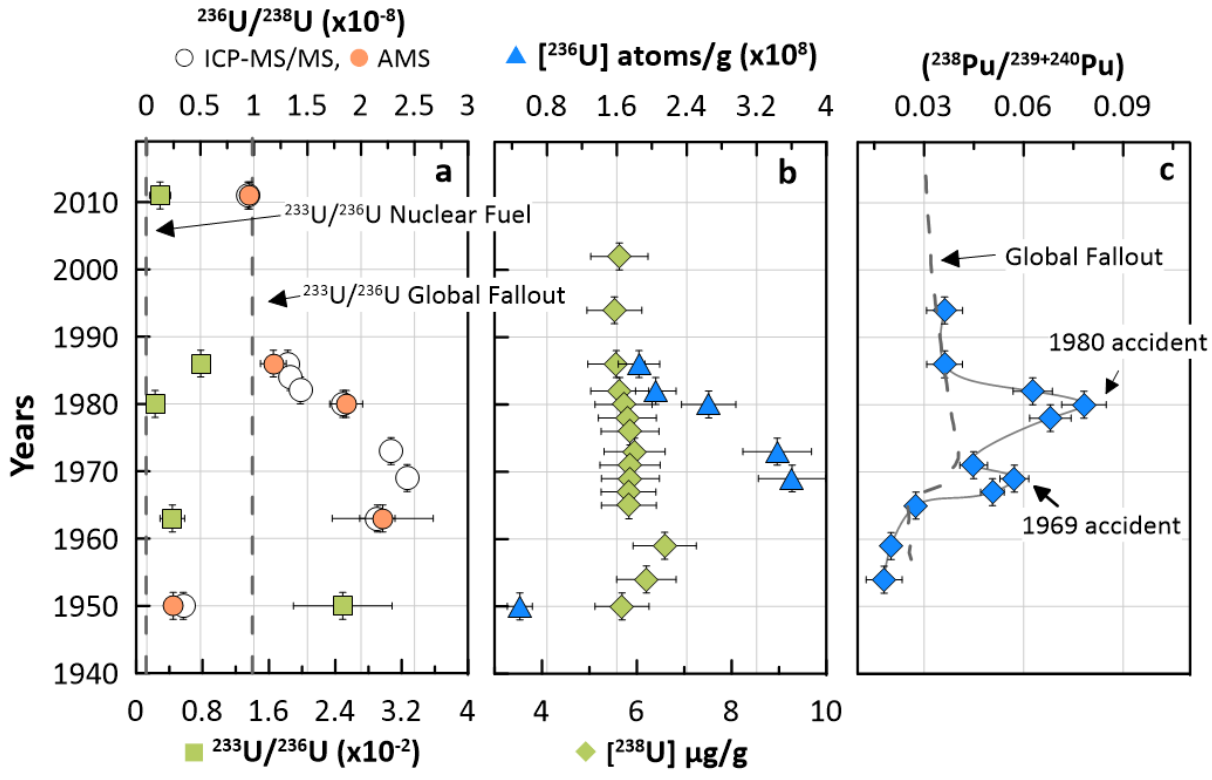

Figure 2: Sediment core profiles of: a) $^{236}U/^{238}U$ and $^{233}U/^{236}U$ isotope ratios, b) ^{238}U and ^{236}U concentrations and c) ($^{238}Pu/^{239+240}Pu$) activity ratios , modified from Eyrolle et al. (2019). The three dashed lines indicate the $^{233}U/^{236}U$ average ratios for the spent nuclear fuel and global fallout (Hain et al., 2020) (a) and the average ($^{238}Pu/^{239+240}Pu$) activity ratios for the global fallout Eyrolle et al. (2019) (c). Uncertainties are expressed for a coverage factor k=2 and when they are not visible, are included in the points.

Investigating the impact of the U-mining and milling activities using stable Pb isotope ratio.

Lead isotope ratios were plotted in a three isotope diagram (Figure 3) in which three end-members were represented: the PDAC (Stacey and Kramers, 1975), the gasoline emissions in France (Monna et al., 1997) and the U-ores from France. For the calculation of the U-ore end-member an age of ≈ 280 Ma, corresponding to an average value of the U deposition in the Loire watershed and in particular in the study area, was used (Cathelineau et al., 1990). This age leads to a radiogenic $^{206}Pb/^{207}Pb$ end-member equal to 19.27. As can be seen in Figure 3, the good alignment of the samples confirms a binary mixing between the Pb from the PDAC and the Pb from gasoline emissions without any significant influence from the U-mining and milling activities. This finding is in agreement with previous works in the Loire River showing an important influence of Pb from gasoline emissions (Négrel and Petelet-Giraud, 2012). As radiogenic Pb is rather associated with particulate bearing phases, the fact that no Pb marked by the U-ore signature was found highlights that U-mining material dissemination was probably limited closer to mining sites (e.g. in (Cuvier et al., 2016; Gourgiotis et al., 2020; Martin et al., 2020)). For this reason coring the sub-watershed of the former U-mines may be more relevant to highlight signatures of U ore and associated mining activities in sediments. This isotopic study shows that U-bearing minerals are poorly transported during sedimentary cascade in the Loire basin.

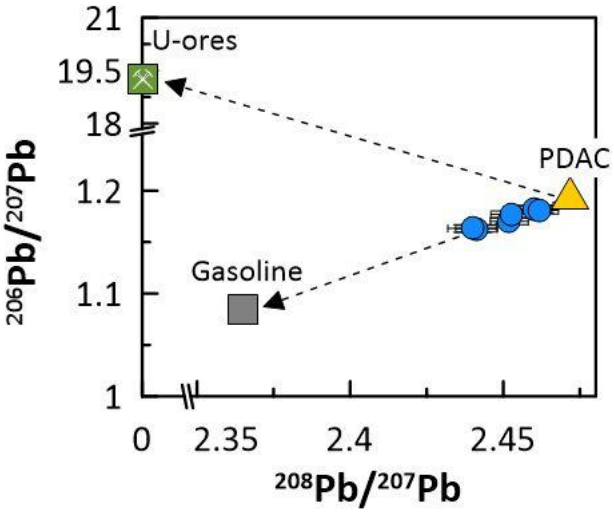

Figure 3: Lead isotope ratio measured in the sediment core collected in the Loire River (blue dots) in a three isotope plot. For the gasoline (grey square) and the geochemical background (PDAC) endmembers, the values of Monna et al. (1997) and Stacey and Kramers (1975) were used, respectively. For the U-ore endmember a ratio of $^{206}Pb/^{207}Pb$ equal to 19.27 was used corresponding to an average age of ≈ 280 Ma (Cathelineau et al., 1990).

In Figure 4 the decrease of the $^{206}Pb/^{207}Pb$ ratio between 1959 and 1986 highlights the increasing use of lead in gasoline (Ayrault et al., 2012; Monna et al., 1997). Considering the $^{206}Pb/^{207}Pb$ ratio dated back to 1950 as the reference value (sediments not or slightly influenced by gasoline-derived Pb),

ratio values in recent years return back to the reference value pointing probably out the resilience time of the system.

A binary mixing model taking into account the atomic abundances of Pb (Gourgiotis et al., 2020) has been used to determine the proportion of lead from gasoline:

$$Ab^{206}_{sample} = kAb^{206}_{gasoline} + (1-k)Ab^{206}_{background}$$

Where Ab^{206} are the ^{206}Pb atomic abundances of the sample, gasoline and geochemical background, respectively. For the gasoline and the geochemical background end-members the values of Monna et al. (1997) and of the core layer dated back to 1950 were used, respectively. Knowing these abundances, the *k* factor that expresses the proportion of the gasoline Pb to the Pb of the sample can be calculated. Results of this mixing model show that the gasoline contribution is about 1% in 1959 and increases over time: 11% in 1963 15% in 1980 and 16% in 1986. In 2011, the ^{206}Pb/^{207}Pb ratio reaches the local geochemical background value, showing a resiliency of the system following the progressive replacing of leaded gasoline by unleaded gasoline, since 1990 in France. Indeed, the release of leaded gasoline in the atmosphere started decreasing around 1990 in France (Lestel et al., 2007)

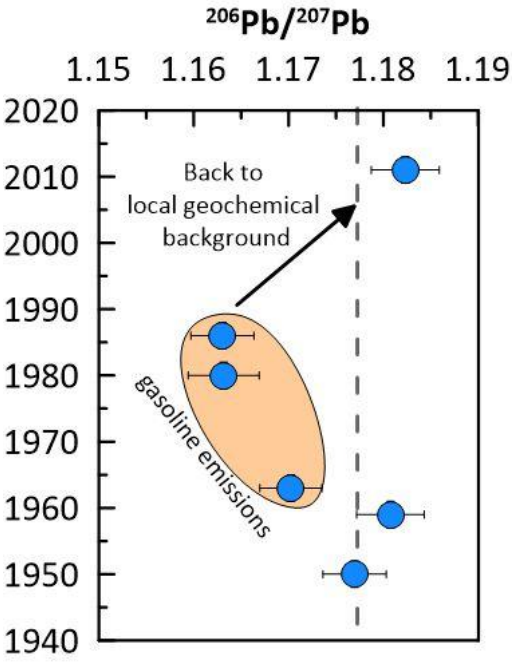

Figure 4: Profile of ^{206}Pb/^{207}Pb isotopic ratio measured in the sediment core collected in the Loire River. The dashed line corresponds to the ratio value dated back to 1950 considered as the local geochemical background value.

Conclusions

The first records of ^{233}U and ^{236}U in a well dated sedimentary archive collected in the Loire River were presented. Thanks to the recent capabilities of ultra-trace level measurements of ^{236}U and in particular ^{233}U, different potential sources of anthropogenic U transiting in the Loire River since the 1950s were discussed. This work confirms the high sensitivity of the $^{236}U/^{238}U$ ratio to highlight small anthropogenic inputs for which the naturally occurring U isotopes are completely "blind". However, the very low levels of ^{236}U in the samples made the identification of the emission sources quite tricky. The recently developed $^{233}U/^{236}U$ tracer combining two anthropogenic isotopes, has made it possible to further consider NPP accident contributions *versus* the global fallout of ^{236}U. These observations are consistent with the ($^{238}Pu/^{239+240}Pu$) activity ratio peaks in 1969 and 1980. However, future studies are needed to profoundly explore the NPPs $^{233}U/^{236}U$ ratio signature, e.g. by analyzing surface sediments and river water from the vicinity of different NPPs, in combination with data related to fuel source terms. The determination of the mining activities by the use of stable Pb isotopes is still challenging probably due to the limited dissemination of the Pb-bearing material marked by the U-ore signature downstream to the former U mines. However, thanks to the lead isotopes the impact of the gasoline atmospheric emissions was clearly highlighted and estimated. Further research is needed to identify the impact of mining and milling activities in the Loire River sediments involving new coring of the sub-watershed of the former U-mines and / or the use of additional relevant tracers (isotopic and elemental).

Acknowledgements

The authors are grateful to the Institute for Radioprotection and Nuclear Safety (France), the NEEDS-Environment fundings (PALYNO project, 2017-2018) and the ANR TRAJECTOIRE project (ANR-19-CE3-0009, 2020-2024) and its team for supporting this work. The authors warmly thank Jean-Paul Bakyono, Franck Giner, David Mourier, Xavier Cagnat and Anne De Vismes for their precious help for field operation, sample preparation and sample analyses. This is PATERSON, the IRSN mass spectrometry platform, contribution n°13.

References

Alam, M.F., Hu, J., Yang, G., Ullah, A.K.M.A., Khalil, M.I., Kibria, A.K.M.F., Rahman, I.M.M., Nanba, K., Yamada, M., 2021. First study on ^{236}U in environmental samples from Bangladesh by ICP-MS/MS prior to the operation of its first nuclear power plant. Journal of Radioanalytical and Nuclear Chemistry. https://doi.org/10.1007/s10967-021-07931-5

Ayrault, S., Roy-Barman, M., Le Cloarec, M.-F., Priadi, C.R., Bonté, P., Göpel, C., 2012. Lead contamination of the Seine River, France: Geochemical implications of a historical perspective. Chemosphere 87, 902–910. https://doi.org/10.1016/j.chemosphere.2012.01.043

Bollhöfer, A., 2012. Stable lead isotope ratios and metals in freshwater mussels from a uranium mining environment in Australia's wet-dry tropics. Applied Geochemistry 27, 171–185. https://doi.org/10.1016/j.apgeochem.2011.10.002

Bollhöfer, A., Honeybun, R., Rosman, K., Martin, P., 2006. The lead isotopic composition of dust in the vicinity of a uranium mine in northern Australia and its use for radiation dose assessment. Science of The Total Environment 366, 579–589. https://doi.org/10.1016/j.scitotenv.2005.11.016

Bollhöfer, A., Martin, P., 2003. Radioactive and Radiogenic Isotopes in Ngarradj (Swift Creek) Sediments: A Baseline Study. Department of the Environment and Heritage, Internal Report 404.

Bouisset, P., Calmet, D., 1997. Hyper pure gamma-ray spectrometry applied to low-level environmental sample measurements. Esarda report EUR 17312 (1997) 73-81 Workshop on the status of measurement techniques for the identification of nuclear signatures, Geel, belgium, 25-27/02/1997.

Boulyga, S.F., Becker, J.S., 2001. Determination of uranium isotopic composition and ^{236}U content of soil samples and hot particles using inductively coupled plasma mass spectrometry. Fresenius' Journal of Analytical Chemistry 370, 612–617. https://doi.org/10.1007/s002160100838

Casacuberta, N., Christl, M., Lachner, J., van der Loeff, M.R., Masqué, P., Synal, H.A., 2014. A first transect of ^{236}U in the North Atlantic Ocean. Geochimica et Cosmochimica Acta 133, 34–46. https://doi.org/10.1016/j.gca.2014.02.012

Cathelineau, M., Boiron, M.C., Holliger, P., Poty, B., 1990. Metallogenesis of the French part of the Variscan orogen. Part II: Time-space relationships between U, Au and Sn-W ore deposition and geodynamic events — mineralogical and U-Pb data. Tectonophysics 177, 59–79. https://doi.org/10.1016/0040-1951(90)90274-C

Child, D.P., Hotchkis, M.A.C., 2013. Plutonium and uranium contamination in soils from former nuclear weapon test sites in Australia. Nuclear Instruments and Methods in Physics Research Section B: Beam Interactions with Materials and Atoms 294, 642–646. https://doi.org/10.1016/j.nimb.2012.05.018

Christl, M., Casacuberta, N., Lachner, J., Maxeiner, S., Vockenhuber, C., Synal, H.-A., Goroncy, I., Herrmann, J., Daraoui, A., Walther, C., Michel, R., 2015. Status of ^{236}U analyses at ETH Zurich and the distribution of ^{236}U and ^{129}I in the North Sea in 2009. Nuclear Instruments and Methods in Physics Research Section B: Beam Interactions with Materials and Atoms 361, 510–516. https://doi.org/10.1016/j.nimb.2015.01.005

Copard, Y., Eyrolle, F., Grosbois, C., Lepage, H., Ducros, L., Morereau, A., Bodereau, N., Cossonnet, C., Desmet, M., 2021. The unravelling of radiocarbon composition of organic carbon in river sediments to document past anthropogenic impacts on river systems. Science of The Total Environment 150890. https://doi.org/10.1016/j.scitotenv.2021.150890

Coularis, C., 2016. Dynamic and transfer of carbon in Loire watershed using carbon isotopes. Thèse de doctorat. Université Paris Saclay (COmUE).

Cumming, G.L., Richards, J.R., 1975. Ore lead isotope ratios in a continuously changing earth. Earth and Planetary Science Letters 28, 155–171. https://doi.org/10.1016/0012-821X(75)90223-X

Cuvier, A., Pourcelot, L., Probst, A., Prunier, J., Le Roux, G., 2016. Trace elements and Pb isotopes in soils and sediments impacted by uranium mining. Science of The Total Environment 566–567, 238–249. https://doi.org/10.1016/j.scitotenv.2016.04.213

Dang, D.H., Wang, W., Pelletier, P., Poulain, A.J., Evans, R.D., 2018. Uranium dispersion from U tailings and mechanisms leading to U accumulation in sediments: Insights from biogeochemical and isotopic approaches. Science of The Total Environment 610–611, 880–891. https://doi.org/10.1016/j.scitotenv.2017.08.156

Dhivert, E., 2014. Mécanismes et modalités de la distribution spatiale et temporelle des métaux dans les sédiments du bassin versant de la Loire.

Douville, E., Sallé, E., Frank, N., Eisele, M., Pons-Branchu, E., Ayrault, S., 2010. Rapid and accurate U–Th dating of ancient carbonates using inductively coupled plasma-quadrupole mass spectrometry. Chemical Geology 272, 1–11. https://doi.org/10.1016/j.chemgeo.2010.01.007

Eyrolle, F., Copard, Y., Lepage, H., Ducros, L., Morereau, A., Grosbois, C., Cossonnet, C., Gurriaran, R., Booth, S., Desmet, M., 2019. Evidence for tritium persistence as organically bound forms in river sediments since the past nuclear weapon tests. Sci Rep 9, 11487. https://doi.org/10.1038/s41598-019-47821-1

Frostick, A., Bollhöfer, A., Parry, D., 2011. A study of radionuclides, metals and stable lead isotope ratios in sediments and soils in the vicinity of natural U-mineralisation areas in the Northern Territory. Journal of Environmental Radioactivity 102, 911–918. https://doi.org/10.1016/j.jenvrad.2010.04.003

Frostick, A., Bollhöfer, A., Parry, D., Munksgaard, N., Evans, K., 2008. Radioactive and radiogenic isotopes in sediments from Cooper Creek, Western Arnhem Land. Journal of Environmental Radioactivity 99, 468–482. https://doi.org/10.1016/j.jenvrad.2007.08.015

Gourgiotis, A., Mangeret, A., Manhès, G., Blanchart, P., Stetten, L., Morin, G., Le Pape, P., Lefebvre, P., Le Coz, M., Cazala, C., 2020. New Insights into Pb Isotope Fingerprinting of U-Mine Material Dissemination in the Environment: Pb Isotopes as a Memory Dissemination Tracer. Environ. Sci. Technol. 54, 797–806. https://doi.org/10.1021/acs.est.9b04828

Grosbois, C., Meybeck, M., Lestel, L., Lefèvre, I., Moatar, F., 2012. Severe and contrasted polymetallic contamination patterns (1900–2009) in the Loire River sediments (France). Science of The Total Environment 435–436, 290–305. https://doi.org/10.1016/j.scitotenv.2012.06.056

Guignard, P., Catoire, S., 2015. Les incidents et accidents nucléaires dans la centrale de Saint-Laurent-des-Eaux sur les réacteurs uranium naturel – graphite – gaz. https://www.vie-publique.fr/sites/default/files/rapport/pdf/164000355.pdf.

Gulson, B.L., Mizon, K.J., Korsch, M.J., Noller, B.N., 1989. Lead isotopes as seepage indicators around a uranium tailings dam. Environ. Sci. Technol. 23, 290–294. https://doi.org/10.1021/es00180a004

Hain, K., Steier, P., Eigl, R., Froehlich, M.B., Golser, R., Hou, X., Lachner, J., Qiao, J., Quinto, F., Sakaguchi A, 2017. $^{233}U/^{236}U$ – A new tracer for environmental processes? Abstract from 4th International Conference on Environmental Radioactivity, Vilnius, Lithuania.

Hain, K., Steier, P., Froehlich, M.B., Golser, R., Hou, X., Lachner, J., Nomura, T., Qiao, J., Quinto, F., Sakaguchi, A., 2020. $^{233}U/^{236}U$ signature allows to distinguish environmental emissions of civil nuclear industry from weapons fallout. Nat Commun 11, 1275. https://doi.org/10.1038/s41467-020-15008-2

Hotchkis, M.A.C., Child, D., Fink, D., Jacobsen, G.E., Lee, P.J., Mino, N., Smith, A.M., Tuniz, C., 2000. Measurement of ^{236}U in environmental media. Nuclear Instruments and Methods in Physics Research Section B: Beam Interactions with Materials and Atoms 172, 659–665. https://doi.org/10.1016/S0168-583X(00)00146-4

Ielsch, G., Cuney, M., Buscail, F., Rossi, F., Leon, A., Cushing, M.E., 2017. Estimation and mapping of uranium content of geological units in France. Journal of Environmental Radioactivity 166, 210–219. https://doi.org/10.1016/j.jenvrad.2016.05.022

IRSN, 2019. IRSN MIMAUSA database, Memory and Impact of uranium mines: synthesis and records, June 2019, https://mimausabdd.irsn.fr/.

IRSN, 2016. Rejets de plutonium dans la Loire Recherche d'un marquage historique au sein d'une archive sédimentaire collectée le 21 juillet 2015 à Montjean-sur-Loire. https://www.irsn.fr/FR/Actualites_presse/Actualites/Documents/IRSN_NI_Rejets-plutonium-Loire_17032016.pdf.

Jaegler, H., Gourgiotis, A., Steier, P., Golser, R., Diez, O., Cazala, C., 2020. Pushing Limits of ICP–MS/MS for the Determination of Ultralow ^{236}U/ ^{238}U Isotope Ratios. Anal. Chem. 92, 7869–7876. https://doi.org/10.1021/acs.analchem.0c01121

Jaegler, H., Pointurier, F., Diez-Fernández, S., Gourgiotis, A., Isnard, H., Hayashi, S., Tsuji, H., Onda, Y., Hubert, A., Laceby, J.P., Evrard, O., 2019. Reconstruction of uranium and plutonium isotopic signatures in sediment accumulated in the Mano Dam reservoir, Japan, before and after the Fukushima nuclear accident. Chemosphere 225, 849–858. https://doi.org/10.1016/j.chemosphere.2019.03.064

Ketterer, M.E., Hafer, K.M., Link, C.L., Royden, C.S., Hartsock, W.J., 2003. Anthropogenic ^{236}U at Rocky Flats, Ashtabula river harbor, and Mersey estuary: three case studies by sector inductively coupled plasma mass spectrometry. Journal of Environmental Radioactivity 67, 191–206. https://doi.org/10.1016/S0265-931X(02)00186-8

Kister, P., Cuney, M., Golubev, V.N., Royer, J.-J., Le Carlier De Veslud, C., Rippert, J.-C., 2004. Radiogenic lead mobility in the Shea Creek unconformity-related uranium deposit (Saskatchewan, Canada): migration pathways and Pb loss quantification. Comptes Rendus Geoscience 336, 205–215. https://doi.org/10.1016/j.crte.2003.11.006

Komárek, M., Ettler, V., Chrastný, V., Mihaljevič, M., 2008. Lead isotopes in environmental sciences: A review. Environment International 34, 562–577. https://doi.org/10.1016/j.envint.2007.10.005

Kyser, K., Lahusen, L., Drever, G., Dunn, C., Leduc, E., Chipley, D., 2015. Using Pb isotopes in surface media to distinguish anthropogenic sources from undercover uranium sources. Comptes Rendus Geoscience 347, 215–226. https://doi.org/10.1016/j.crte.2015.06.003

Lestel, L., Meybeck, M., Thévenot, D.R., 2007. Metal contamination budget at the river basin scale: an original Flux-Flow Analysis (F2A) for the Seine River. Hydrol. Earth Syst. Sci. 11, 1771–1781. https://doi.org/10.5194/hess-11-1771-2007

Lin, M., Qiao, J., Hou, X., Dellwig, O., Steier, P., Hain, K., Golser, R., Zhu, L., 2021. 70-Year Anthropogenic Uranium Imprints of Nuclear Activities in Baltic Sea Sediments. Environ. Sci. Technol. acs.est.1c02136. https://doi.org/10.1021/acs.est.1c02136

Liu, J., Luo, X., Wang, J., Xiao, T., Yin, M., Belshaw, N.S., Lippold, H., Kong, L., Xiao, E., Bao, Z., Li, N., Chen, Y., Linghu, W., 2018. Provenance of uranium in a sediment core from a natural reservoir, South China: Application of Pb stable isotope analysis. Chemosphere 193, 1172–1180. https://doi.org/10.1016/j.chemosphere.2017.11.131

Liu, Z., Hu, J., Yamada, M., Yang, G., 2020. Uranium and plutonium isotopes and their environmental implications in surface sediments from the Yangtze River catchment and estuary. CATENA 193, 104605. https://doi.org/10.1016/j.catena.2020.104605

Manhes, G., Allegre, C.J., Provost, A., 1984. U-Th-Pb systematics of the eucrite "Juvinas": Precise age determination and evidence for exotic lead. Geochimica et Cosmochimica Acta 48, 2247–2264. https://doi.org/10.1016/0016-7037(84)90221-7

Marsden, O.J., Livens, F.R., Day, J.P., Fifield, L.K., Goodall, P.S., 2001. Determination of U-236 in sediment samples by accelerator mass spectrometry. Analyst 126, 633–636. https://doi.org/10.1039/b009764k

Martin, A., Hassan-Loni, Y., Fichtner, A., Péron, O., David, K., Chardon, P., Larrue, S., Gourgiotis, A., Sachs, S., Arnold, T., Grambow, B., Stumpf, T., Montavon, G., 2020. An integrated approach combining soil profile, records and tree ring analysis to identify the origin of environmental contamination in a former uranium mine (Rophin, France). Science of The Total Environment 747, 141295. https://doi.org/10.1016/j.scitotenv.2020.141295

Mikhailov, V.N., Andryushin, L.A., Voloshin, N.P., Ilkaev, R.I., Matushchenko, A.M., Ryabev, L.D., Strukov, V.G., Chernyshev, A.K., Yudin, Yu.A., 1999. Catalog of worldwide nuclear testing, by Begell-Atom. begell-atom, llc 1–56700.

Mironov, V.P., Matusevich, J.L., Kudrjashov, V.P., Boulyga, S.F., Becker, J.S., 2002. Determination of irradiated reactor uranium in soil samples in Belarus using ^{236}U as irradiated uranium tracer. Journal of Environmental Monitoring 4, 997–1002. https://doi.org/10.1039/b207573c

Monna, F., Lancelot, J., Croudace, I.W., Cundy, A.B., Lewis, J.T., 1997. Pb Isotopic Composition of Airborne Particulate Material from France and the Southern United Kingdom: Implications for Pb Pollution Sources in Urban Areas. Environmental Science & Technology 31, 2277–2286. https://doi.org/10.1021/es960870+

Morereau, A., 2020. Reconstitution à partir d'archives sédimentaires des concentrations et des sources des radionucléides ayant transité dans le Rhône et la Loire au cours de l'ère nucléaire (Thèse de doctorat). Aix-Marseille Université.

Munksgaard, N.C., Brazier, J.A., Moir, C.M., Parry, D.L., 2003. The Use of Lead Isotopes in Monitoring Environmental Impacts of Uranium and Lead Mining in Northern Australia. Australian journal of chemistry 56, 233–238. https://doi.org/10.1071/CH02239

Naegeli, R., 2004. Calculation of the radionuclides in PWR spent fuel samples for SFR experiment planning. (No. SAND2004-2757, 919122). https://doi.org/10.2172/919122

Négrel, P., Petelet-Giraud, E., 2012. Isotopic evidence of lead sources in Loire River sediment. Applied Geochemistry 27, 2019–2030. https://doi.org/10.1016/j.apgeochem.2012.05.015

Patterson, C.C, Settle, D.M., 1987. Review of data on eolian fluxes of industrial and natural lead to the lands and seas in remote regions on a global scale. Marine Chemistry 22, 137–162. https://doi.org/10.1016/0304-4203(87)90005-3

Patterson, Clair C, Settle, D.M., 1987. Magnitude of lead flux to the atmosphere from volcanoes. Geochimica et Cosmochimica Acta 51, 675–681. https://doi.org/10.1016/0016-7037(87)90078-0

Qiao, J., Ransby, D., Steier, P., 2022. Deciphering anthropogenic uranium sources in the equatorial northwest Pacific margin. Science of The Total Environment 806, 150482. https://doi.org/10.1016/j.scitotenv.2021.150482

Qiao, J., Zhang, H., Steier, P., Hain, K., Hou, X., Vartti, V.-P., Henderson, G., Eriksson, M., Aldahan, A., Possnert, G., 2020. A previously unknown source of reactor radionuclides in the Baltic Sea, identified by ^{233}, ^{23}6, ^{238}U and ^{127}, ^{129}I multi-fingerprinting (preprint). In Review. https://doi.org/10.21203/rs.3.rs-49352/v1

Qiao, J., Zhang, H., Steier, P., Hain, K., Hou, X., Vartti, V.-P., Henderson, G.M., Eriksson, M., Aldahan, A., Possnert, G., Golser, R., 2021. An unknown source of reactor radionuclides in the Baltic Sea revealed by multi-isotope fingerprints. Nat Commun 12, 823. https://doi.org/10.1038/s41467-021-21059-w

Quinto, F., Hrnecek, E., Krachler, M., Shotyk, W., Steier, P., Winkler, S.R., 2013. Measurements of ^{236}U in Ancient and Modern Peat Samples and Implications for Postdepositional Migration of Fallout Radionuclides. Environmental Science & Technology 47, 5243–5250. https://doi.org/10.1021/es400026m

Quinto, F., Steier, P., Wallner, G., Wallner, A., Srncik, M., Bichler, M., Kutschera, W., Terrasi, F., Petraglia, A., Sabbarese, C., 2009. The first use of ^{236}U in the general environment and near a shutdown nuclear power plant. Applied Radiation and Isotopes 67, 1775–1780. https://doi.org/10.1016/j.apradiso.2009.05.007

Sakaguchi, A., Kadokura, A., Steier, P., Takahashi, Y., Shizuma, K., Hoshi, M., Nakakuki, T., Yamamoto, M., 2012. Uranium-236 as a new oceanic tracer: A first depth profile in the Japan Sea and comparison with caesium-137. Earth and Planetary Science Letters 333–334, 165–170. https://doi.org/10.1016/j.epsl.2012.04.004

Sakaguchi, A., Kawai, K., Steier, P., Imanaka, T., Hoshi, M., Endo, S., Zhumadilov, K., Yamamoto, M., 2010. Feasibility of using ^{236}U to reconstruct close-in fallout deposition from the Hiroshima

atomic bomb. Science of The Total Environment 408, 5392–5398. http://dx.doi.org/10.1016/j.scitotenv.2010.07.073

Sakaguchi, A., Kawai, K., Steier, P., Quinto, F., Mino, K., Tomita, J., Hoshi, M., Whitehead, N., Yamamoto, M., 2009. First results on ^{236}U levels in global fallout. Science of The Total Environment 407, 4238–4242. http://dx.doi.org/10.1016/j.scitotenv.2009.01.058

Sakaguchi, A., Steier, P., Takahashi, Y., Yamamoto, M., 2014. Isotopic Compositions of ^{236}U and Pu Isotopes in "Black Substances" Collected from Roadsides in Fukushima Prefecture: Fallout from the Fukushima Dai-ichi Nuclear Power Plant Accident. Environmental Science & Technology 48, 3691–3697. https://doi.org/10.1021/es405294s

Santos, R.M.P., Tassinari, C.C.G., 2012. Different lead sources in an abandoned uranium mine (Urgeiriça - Central Portugal) and its environment impact – isotopic evidence. Geochemistry: Exploration, Environment, Analysis 12, 241–252. https://doi.org/10.1144/1467-7873/11-ra-076

Shao, Y., Yang, G., Xu, D., Yamada, M., Tazoe, H., Luo, M., Cheng, H., Yang, K., Ma, L., 2019. First report on global fallout ^{236}U and uranium atom ratios in soils from Hunan Province, China. Journal of Environmental Radioactivity 197, 1–8. https://doi.org/10.1016/j.jenvrad.2018.11.009

Shinonaga, T., Steier, P., Lagos, M., Ohkura, T., 2014. Airborne Plutonium and Non-Natural Uranium from the Fukushima DNPP Found at 120 km Distance a Few Days after Reactor Hydrogen Explosions. Environmental Science & Technology 48, 3808–3814. https://doi.org/10.1021/es404961w

Srncik, M., Hrnecek, E., Steier, P., Wallner, G., 2011a. Determination of U, Pu and Am isotopes in Irish Sea sediment by a combination of AMS and radiometric methods. Journal of Environmental Radioactivity 102, 331–335. https://doi.org/10.1016/j.jenvrad.2011.01.004

Srncik, M., Steier, P., Wallner, G., 2011b. Depth profile of ^{236}U/^{238}U in soil samples in La Palma, Canary Islands. Journal of Environmental Radioactivity 102, 614–619. https://doi.org/10.1016/j.jenvrad.2011.03.011

Stacey, J.S., Kramers, J.D., 1975. Approximation of terrestrial lead isotope evolution by a two-stage model. Earth and Planetary Science Letters 26, 207–221. https://doi.org/10.1016/0012-821X(75)90088-6

Steier, P., Bichler, M., Keith Fifield, L., Golser, R., Kutschera, W., Priller, A., Quinto, F., Richter, S., Srncik, M., Terrasi, P., Wacker, L., Wallner, A., Wallner, G., Wilcken, K.M., Maria Wild, E., 2008. Natural and anthropogenic ^{236}U in environmental samples. Nuclear Instruments and Methods in Physics Research Section B: Beam Interactions with Materials and Atoms 266, 2246–2250. https://doi.org/10.1016/j.nimb.2008.03.002

Steier, P., Hain, K., Klötzli, U., Lachner, J., Priller, A., Winkler, S., Golser, R., 2019. The actinide beamline at VERA. Nuclear Instruments and Methods in Physics Research Section B: Beam Interactions with Materials and Atoms 458, 82–89. https://doi.org/10.1016/j.nimb.2019.07.031

Thomas, A.J., 1982. Comportement géochimique des radionucléides a l'amont de l'estuaire de la Loire. PhD, https://archimer.ifremer.fr/doc/00106/21685/.

Tumey, S.J., Brown, T.A., Buchholz, B.A., Hamilton, T.F., Hutcheon, I.D., Williams, R.W., 2009. Ultra-sensitive measurements of ^{233}U by accelerator mass spectrometry for national security applications. Journal of Radioanalytical and Nuclear Chemistry 282, 721. https://doi.org/10.1007/s10967-009-0332-z

Vecchia, A.M.D., Rodrigues, P.C.H., Rios, F.J., Ladeira, A.C.Q., 2017. Investigations into Pb isotope signatures in groundwater and sediments in a uranium-mineralized area. Brazilian journal of geology 47, 147–158. https://doi.org/10.1590/2317-4889201720160100

Wang, Y., Hou, X., Zhang, W., Zhang, L., Fan, Y., 2021. Determination of ultra-low ^{236}U in environment samples using ICP-MS/MS measurement and chemical separation. Talanta 224, 121882. https://doi.org/10.1016/j.talanta.2020.121882

690 Wilcken, K.M., Fifield, L.K., Barrows, T.T., Tims, S.G., Gladkis, L.G., 2008. Nucleogenic ^{36}Cl, ^{236}U and
691 ^{239}Pu in uranium ores. Nuclear Instruments and Methods in Physics Research Section B: Beam
692 Interactions with Materials and Atoms 266, 3614–3624.
693 https://doi.org/10.1016/j.nimb.2008.06.009
694 Yang, G., Rahman, M.S., Tazoe, H., Hu, J., Shao, Y., Yamada, M., 2019. ^{236}U and radiocesium in river
695 bank soil and river sediment in Fukushima Prefecture, after the Fukushima Daiichi Nuclear
696 Power Plant accident. Chemosphere 225, 388–394.
697 https://doi.org/10.1016/j.chemosphere.2019.03.061
698 Yang, G., Tazoe, H., Yamada, M., 2016. Determination of ^{236}U in environmental samples by single
699 extraction chromatography coupled to triple-quadrupole inductively coupled plasma-mass
700 spectrometry. Analytica Chimica Acta 944, 44–50. https://doi.org/10.1016/j.aca.2016.09.033
701